FEL experiments at sparc: Operation in seeded and chirped mode

Conference Paper · September 2010

CITATIONS
2

READS
49

51 authors, including:

L. Giannessi
ENEA
381 PUBLICATIONS **3,243** CITATIONS
SEE PROFILE

Alberto Petralia
ENEA
72 PUBLICATIONS **491** CITATIONS
SEE PROFILE

Giuseppe Dattoli
ENEA
900 PUBLICATIONS **6,958** CITATIONS
SEE PROFILE

Franco Ciocci
ENEA
152 PUBLICATIONS **1,144** CITATIONS
SEE PROFILE

FEL EXPERIMENTS AT SPARC: OPERATION IN SEEDED AND CHIRPED MODE

L. Giannessi, A. Petralia, G. Dattoli, F. Ciocci, M. Del Franco, M. Quattromini, C. Ronsivalle, E. Sabia, I. Spassovsky, V. Surrenti ENEA C.R. Frascati, IT. D. Filippetto, G. Di Pirro, G. Gatti, M. Bellaveglia, D. Alesini, M. Castellano, E. Chiadroni, L. Cultrera, M. Ferrario, L. Ficcadenti, A. Gallo, A, Ghigo, E. Pace, B. Spataro, C. Vaccarezza, INFN-LNF, IT. A. Bacci, V. Petrillo, A.R. Rossi, L. Serafini INFN-MI, IT. M. Serluca, M. Moreno INFN-Roma I, IT. L. Poletto, F. Frassetto CNR-IFN, IT. J.V. Rau, V. Rossi Albertini ISM-CNR, IT. A. Cianchi, UN-Roma II TV, IT. A. Mostacci, M Migliorati, L. Palumbo, Un. Roma La Sapienza, IT. G. Marcus, P. Musumeci, J. Rosenzweig, UCLA, CA, USA. S. Spampinati, ST, IT and University of Nova Gorica, Nova Gorica, M. Labat, F. Briquez, M. E. Couprie, SOLEIL, FR. B. Carré, M. Bougeard, D. Garzella CEA Saclay, DSM/DRECAM, FR. G. Lambert LOA, FR. C.Vicario PSI, CH.

Abstract

We report on the recent activity at SPARC, which has successfully been operated both SASE and seeded mode.

Full SASE has been achieved by combining the velocity bunching compression technique, to increase the peak current, with an undulator tapering, to compensate the chirp in the longitudinal phase space[1].

The seeded mode operation has been accomplished, both as a single amplifier and as a single stage cascade doubling the frequency of the input seed at 400nm. We report on the main results obtained in both the configurations.

INTRODUCTION

The study of FEL dynamics in seeded and cascaded configurations and the FEL operation with exotic beams is central in the scientific program of SPARC [2-3]. In the framework of the DS4 EUROFEL collaboration, a research work plan aiming at the investigation of seeded and cascaded FEL configurations was implemented [3]. The main goal was to study and test the amplification and the FEL harmonic generation process of an input seed signal such as higher order harmonics generated both in crystals and in gases. The SPARC FEL can be configured to test several seeded and cascaded FEL configurations.

In this paper we report on the first seeding experiments exploited at SPARC and on the chirped pulse operation in SASE mode. The paper is organized as follows. In the next section we analyse the FEL operation in seeded mode with the SPARC undulator arranged as a single long amplifier. In Sec. 3 we analyse the results obtained operating the FEL with a single stage HGHG cascaded configuration, with one section tuned at the seed wavelength and five undulators tuned at its second harmonic.

Furthermore the FEL has been recently operated in fully saturated conditions by combining the technique of velocity bunching for increasing the peak current[4], with the idea originally proposed in ref. [1], consisting in tapering the undulator gaps to mitigate the effect of the residual chirp and correlated energy spread resulting from the compression process. Here we report on the quoted results and the last section will be devoted to the analysis of the new features emerging in the chirped-tapering scheme.

SINGLE PASS SEEDED AMPLIFIER

The SPARC FEL is driven by a high brightness accelerator providing a high quality beam at energies between 150 and 200 MeV. The undulator beam line is composed of six, variable gap, undulator sections (See Fig.1).

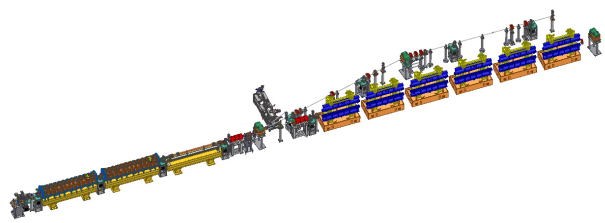

Figure 1: Layout of the SPARC FEL test facility.

A detailed description of the SPARC layout is given in [2,3,4] . The SPARC undulators are variable gap modules of 75 periods each, with a period length of 2.8cm and a maximum K=2.2. Magnetic maps and undulator strength K vs. gap were measured before the undulator installation with a Hall probe mounted on a translation stage. These values were verified with the spontaneous emission spectra measured with a test electron beam, showing a good agreement[5, 6].

The beam transport is obtained with a FODO lattice where quadrupoles in the undulator intersections provide the horizontal focusing and the undulator field provides the vertical focusing. In this condition the matching Twiss β parameter depends on the resonant frequency which sets the undulator field strength. The mean beam energy measured with a magnetic spectrometer installed on the transfer line leading the beam to the undulator is 177.2 MeV. A RF deflector cavity installed on the transfer line before the magnetic spectrometer allows the measure of

the beam parameters as a function of the longitudinal coordinate[7]. The seed used in this experiment is the second harmonics of the Ti:Sa laser, i.e. λ= 401 nm, 120fs FWHM. The seed energy may be increased up to 150μJ but energies below 10μJ were sufficient for the experiments described hereafter. With the undulators tuned at the seed wavelength we match the orbit minimizing the transverse beam size and imposing that the transverse average Twiss β coefficients are the same in the two $\left(\langle\beta_x\rangle=\langle\beta_y\rangle\right)$. With these conditions we have $\langle\beta_x\rangle=\langle\beta_y\rangle\cong 1.5m$. The analysis of the images acquired with the combined use of the deflector cavity and the spectrometer magnet allows the determination of mean energy, energy spread (slice and projected), energy chirp, bunch length and, knowing the bunch charge, measured independently, the longitudinal profile of the bunch current. A list of these parameters is presented in Tab. I.

Table I – Summary of the Main Beam Parameters

Beam energy (MeV)	177.2
Energy Spread (proj., %)	0.13
Energy Spread (slice, %)	0.05
Length (ps - rms)	2.64
Peak current (A)	54
Emittance X (mm mrad)	2.9
Emittance Y (mm mrad)	2.5

An in vacuum spectrometer designed and built by the LUXOR laboratory in Padova is the main radiation diagnostic. The spectrometer gratings and the CCD detector have been calibrated in efficiency and yield to allow the simultaneous determination of spectral properties of the observed radiation and of the single shot pulse energy[8]. The spectra shown in Fig.2 were acquired with all the undulators tuned at 400 nm, after ensuring temporal and spatial superposition between the seed and the electron beam.

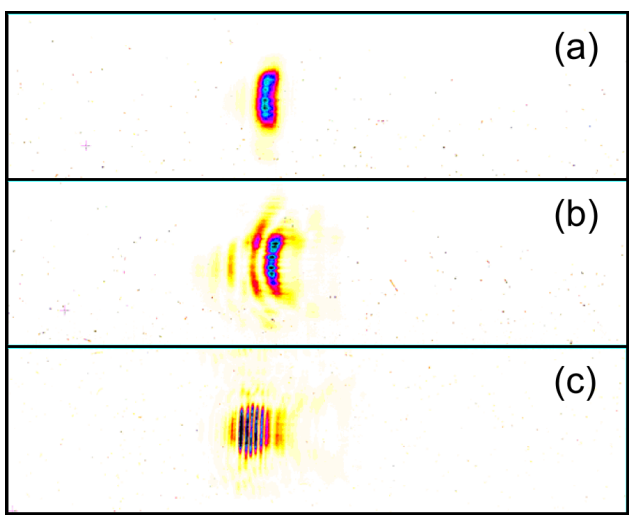

Figure 2: Spectrum of the seeded amplifier. The horizontal axis represents the wavelength, the window range is 45 nm and the central wavelength is 400 nm. The vertical axis indicates the position on the (vertical) entrance slit of the spectrometer. The images with labels (a), (b) and (c) have been obtained with different seed energy: (a) E<0.5μJ , (b) E~3μJ, (c) E~9μJ.

The vertical axis on the image represents the vertical position on the input spectrometer slit, while the horizontal axis represents the wavelength. The window is centred at 400 nm and the represented wavelength range is about 45nm. The figures Fig.2,a to Fig.2,c represent spectra obtained at different seed energy as indicated in the figure caption. The multi-peak structure, corresponding to the presence of various spectral lines, slightly red-shifted compared to the unseeded and HHG is about a factor two larger than the expected SASE bandwidth. The Pierce [9] parameter should be $\rho=3.2\,10^{-3}$, corresponding to a bandwidth of the order of 1.3 nm, while the spectrum in Fig.2.c is larger than 2 nm. The observed pattern, appearing at high seed energy, is completely different both in shape and in intensity from the typical SASE spiking where the number of peaks and their position change from shot to shot. The sidebands structure which appears in the spectrum at high seed energy only, is a saturation effect. This structure may be interpreted as the effect of a saturated pulse slipping forward along the electron pulse, with the radiation emitted by fresh electrons in the pulse front, interfering with radiation out of phase produced by overbunched electrons in the rear part of the pulse. Numerical simulations have been carried out with the GENESIS 1.3 [10-11], implemented with harmonics and with PERSEO Time Dependent code [12] (PTD), taking into account the spectral overlap and three-dimensional effects, such as the transverse mismatch. An amplification of the seed in the exponential regime in the first two sections of the undulator, and superradiance in the other four ones is observed in the simulations. In order to compare the spectra with the simulations the field data generated by GENESIS have been post processed through a numerical procedure resembling the slit/grating/CCD of the spectra detection system.

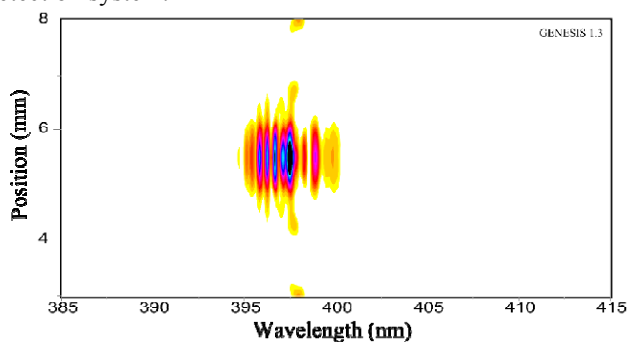

Figure 3: GENESIS 1.3 data, obtained with the following data: I=65A , ε_x=2.9 mm mrad, ε_y=2.5 mm mrad (norm.).

One of the results obtained is shown in Fig. 3 where the spectrum has been deduced from GENESIS 1.3, obtained with the following simulation data: I=65A ,

ε_x=2.9 mm mrad, ε_y=2.5 mm mrad (normalized). The energy per pulse is E =50μJ, to be compared with the energy observed in the experiment E=20μJ with a standard deviation of 6μJ. The energy measured in a sequence of 100 consecutive shots is shown in Fig.4.

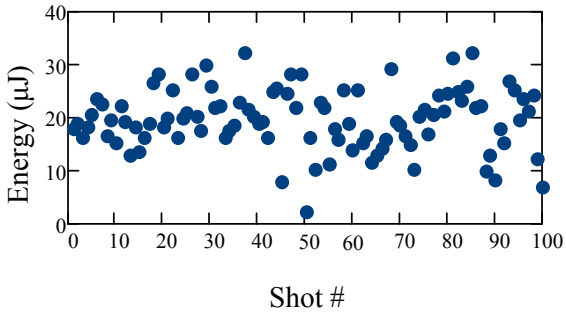

Figure 4: Energy measured in a sequence of 100 consecutive shots.

Harmonics of the fundamental frequency $\lambda_n = \lambda/n$ have been observed up to $n=11$. The spectral emission on the harmonics presents regular Gaussian shape pulse to pulse. In fig. 5 the spectrum from 32 up to 115 nm is shown with the presence of eight harmonics from 11th up to 4th from left (in sequence: 36.18 nm, 39.8nm, 44.2 nm, 49.75 nm, 58.6 nm, 66.3 nm, 79.6 nm, 99.5 nm). Both even and odd harmonics are visible, with the odd ones slightly more intense. In Fig. 6 the spectral band from 115 up to 205.85 is shown with the presence of the second and the third harmonics (132.66 nm and 199 nm). The spatial shape seems to be similar to the unseeded emission.

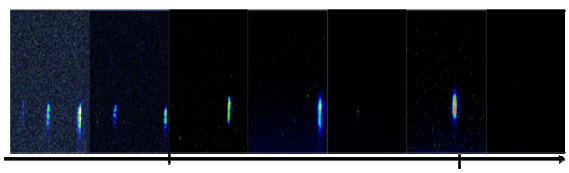

Figure 5: Spectrum from 32 up to 115 nm is shown with the presence of eight harmonics from 11th up to 4th from left (in sequence: 36.18 nm, 39.8nm, 44.2 nm, 49.75 nm, 58.6 nm, 66.3 nm, 79.6 nm, 99.5 nm).

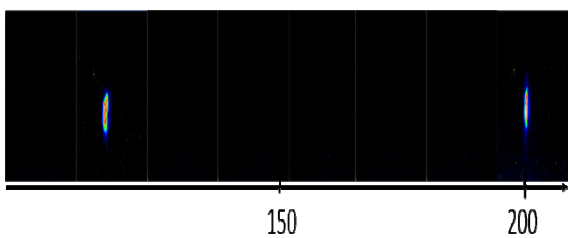

Figure 6: Spectral range from 115 up to 205.85 nm is shown with the presence of the second and the third harmonics (132.66 nm and 199 nm).

The process of coherent higher order harmonics generation in this regime of operation, i.e. with a seed pulse shorter then the e-bunch length was studied in [13]. The regime was originally analysed in ref. [14-16] and explored in a single pass FEL amplification experiment in [17]. It is characterized by a self similar pulse amplified while it propagates through the undulator. The main reason of the expected intense harmonics emission can be found in the structure of the front side of the pulse and in the interaction with the co-propagating electron beam. In Fig. 7a it is shown a plot of the short radiation pulse shifting from left to right because of slippage. In Fig. 7b the expanded view of the electron beam phase space in the pulse front side (colored region in Fig.7a) and the bunching coefficients for the first harmonics, are represented.

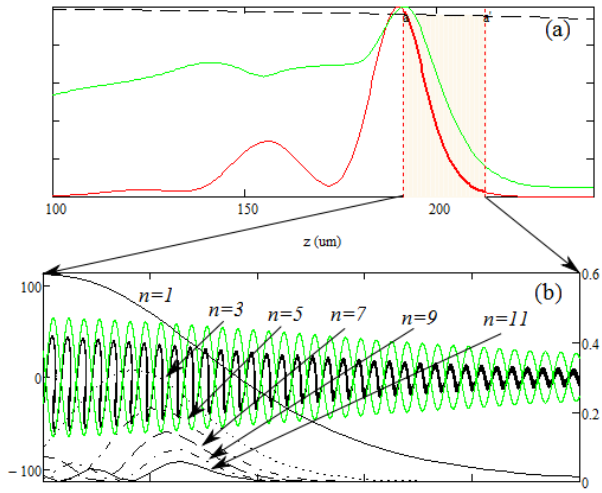

Figure 7: Graphical representation of the radiation pulse slipping from left to right in the e-beam frame (red) and of the induced energy spread (green) (Fig.7a). Longitudinal e-beam phase space in the front part of the pulse (Fig.7b). In Fig.7b the square moduli of the bunching coefficients for the first eleven (odd) harmonics are plotted. The green line represents the motion separatrix whose envelope is proportional to the square root of the laser field (simulation with PERSEO TD).

The pulse advances over fresh electrons on the right side inducing an increasing modulation and bunching. The bunching factor at the fundamental grows from right to left until reaches the maximum value approximately at the peak of the pulse. Bunching factors at the higher order harmonics follow a similar behaviour, reaching the maximum value in a position in the pulse front side with a length scaling as $1/n$. Simulations predict extremely narrow pulses at the highest harmonics. Several aspects of this dynamical regime suggest an intense high harmonics emission. Saturation dynamics is governed by the slippage process. At a given position along the bunch the field grows because of slippage and not because of exponential gain. Fresh electrons are “seeded” by the propagating wave and the faster dynamics in phase space causes the peaks in the bunching coefficients to be narrower with a more effective modulation. The bunching at a given harmonic reaches a maximum value determined by the inhomogeneous dispersion associated to the beam quality. The self similar behaviour of this particular solution of the FEL dynamics causes the fact that the

bunching distribution is "preserved" along the undulator. In steady state regime (or in the long pulse regime), bunching at a given harmonic may be induced over a limited undulator length, because interaction with the laser field and dispersion combined with the induced energy spread, cause debunching. In this particular condition there is a region of the beam phase space, drifting over the electron current where bunching is preserved along the undulator. There is no de-bunching due to dynamics. The experimental observation confirms the predicted behaviour.

SUPERRADIANT CASCADE

Intense short seed pulses allow to test the super-radiant cascade concept [13] where the seed laser power is sufficient to bring the radiation pulse close to saturation in the modulator. The pulse generated in these conditions propagates with the typical signature of superradiance in the next radiators. The six SPARC undulators may be configured in order to set up a single stage cascaded FEL based on a modulator-radiator configuration, similar to the one originally tested at BNL [18]. The layout of this configuration is shown in Fig.8.

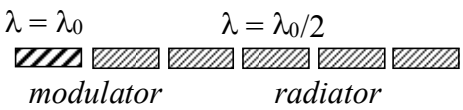

Figure 8: Undulator layout of a single stage cascade at SPARC.

The number of sections playing the role of modulator and radiator may be adjusted to the intensity of the available seed. In conditions similar to the one analysed in the previous section, we have tested the configuration in Fig. 8 composed by a single undulator tuned at 400nm and playing the role of modulator and five undulators tuned at 200 nm as radiators. In Fig. 9 it is shown a plot of the pulse energy measured at 200nm while changing the optical path length of the seed laser. The average, maximum and minimum energy observed in a sequence of 30 shots at each position are plotted. The large difference between the minimum and maximum value of the intensity at a given position was due to a phase jitter of the beam energy which was bringing the seed out of resonance in the modulator.

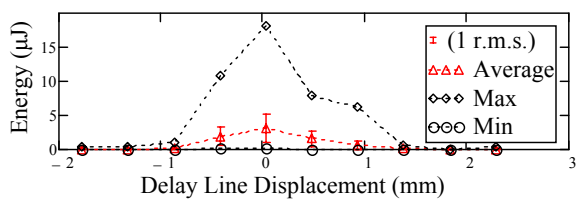

Figure 9: Energy at the exit of the radiator as a function of the relative delay δ between the seed and the electrons in the modulator. The zero position is set to the maximum energy. Error bars represent one standard deviation.

The spectrum at δ=0 corresponding to the shot characterized by the maximum energy is displayed in Fig. 10. The spectrum shows a structure qualitatively similar to the one shown in Fig. 2 suggesting that saturation is reached at this wavelength as well. As in the previous case a significant harmonic emission is expected. The spectrum of the third harmonic of the radiator is shown in Fig. 11 while in Fig. 12 the distribution of energy per pulse and relative linewidth of the third harmonic for a sequence of 30 consecutive spectra is shown. Several shots show energy at the 0.1 μJ level. The large fluctuation of the observed energy is associated to the beam energy jitter which affected the beam during the shift.

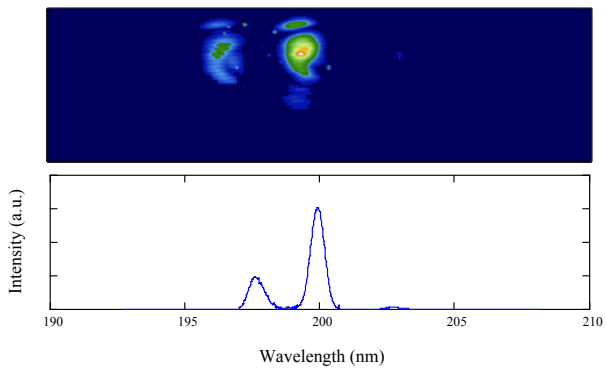

Figure 10: Spectrum of the radiation emitted by the radiator tuned a 200nm.

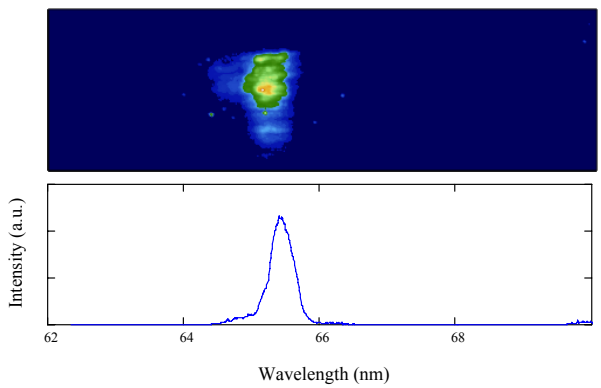

Figure 11: Spectrum of the third harmonic of the radiator.

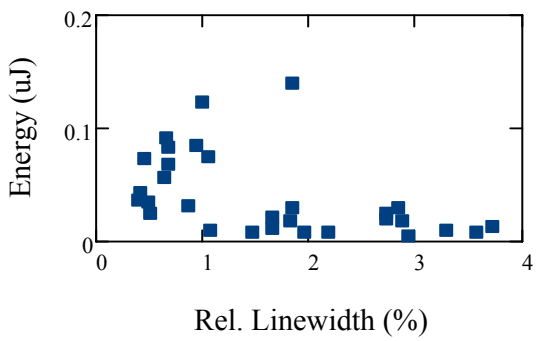

Figure 12: Energy per pulse vs spectral width for a sequence of 30 consecutive spectra.

SASE WITH A CHIRPED BEAM

The SPARC layout, shown in Fig. 1, does not include a magnetic compressor. When the linac is operated in velocity bunching mode, the first linac section is tuned off crest, close to the zero crossing phase. The result is a strong chirp in the longitudinal phase space which leads to an increase of the peak current. This condition has been extensively studied at SPARC [4]. Compression factors up to 17 and compensation of the emittance growth with the superposition of a magnetic field on the first linac section have been demonstrated. The correlated energy spread associated to the chirp would be mitigated in a long linac by longitudinal wakes and by acceleration itself. In the SPARC case the linac is composed of three SLAC type sections only, allowing a maximum energy of about 180MeV. In compression mode, the first section operated out of phase is not optimized for acceleration and the final energy is about 120MeV. The linac structure, typical of an injector, is not sufficient for compensating the correlated energy spread. The phase space at the linac exit still contains a strong residual chirp and despite the high peak current which can be obtained, the detrimental effect of the chirp on the gain prevents the FEL from reaching full saturation.

The effect of the chirp on the gain can be compensated by tapering the undulator. The compensation mechanism can be explained analysing the diagrams shown in Fig.13. The pictures represent the propagation of a field spike (green) developing on the rear part of a chirped e-beam (light blue). The vertical axis represent the resonant condition which depends on the relative position between the beam and the radiation. The upper diagram is relative to the un-tapered case. When the beam propagates through the undulator, the slippage process leads the spike out of resonance. When the chirp is combined with an appropriate undulator taper (lower diagram), the resonance condition can be preserved.

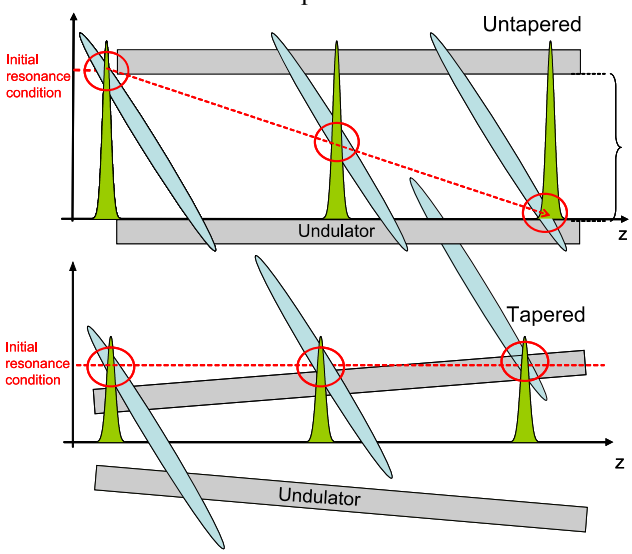

Figure 13: The pictures represent the propagation of a field spike (green) developing on the rear part of a chirped e-beam (light blue). The upper diagram is relevant to the un-tapered case, the lower one to the tapered case.

In a chirped beam the resonant frequency

$$\omega_0 = \frac{2\gamma^2}{1+\frac{K^2}{2}}\omega_u, \qquad \omega_u = 2\pi c/\lambda_u \tag{1}$$

where λ_u is the undulator period, K is the undulator strength and $\gamma = E/m_0c^2$ the beam energy, is a function of the position along the electron bunch. We may define the mean "local" energy as (linear chirp)

$$\gamma(s) = \gamma_0 + \alpha(s - s_0) \tag{2}$$

where s corresponds to the longitudinal coordinate along the electron bunch centred in s_0 in a reference frame drifting at the velocity $\beta_z = 1-\left(1+K^2/2\right)/2\gamma^2$. The parameter α defines the slope of the average slice energy vs. the coordinate s. The different velocity of the light with respect to the electrons brings a radiation spike building up in a given position, out of resonance when it slips of a distance of the order of $\delta s \approx \rho\gamma m_0c^2/2\alpha$. For this reason an inhomogeneous gain broadening associated to energy spread, is expected even with a negligible local energy spread because of slippage. The field in presence of gain propagates at a velocity lower than c, the peak of a spike in the exponential gain regime is expected to move at a velocity given by [16]

$$v_L = \frac{3c\beta_z}{2+\beta_z} \tag{3}$$

Above saturation the front side of the pulse drifts at the velocity of light c. Approaching saturation the radiation peak shifts at a different velocity than (3), closer or even higher than c because of the pulse shortening associated to the electron synchrotron oscillation [19]. A taper of the undulator may be used to compensate the effect of energy dispersion associated to the pulse slippage on the chirped beam [1]. The energy change caused by the chirp and observed at the peak of the radiation pulse may be expressed as

$$\gamma(z) = \gamma_s + \alpha\, z\eta\frac{\omega_u}{\omega_0} \tag{4}$$

where z is the coordinate along the undulator, γ_s is the beam energy at the undulator entrance ($z=0$), at the position along the bunch where the spike will grow, and where η is a coefficient accounting for an arbitrary propagation velocity of the radiation v_L. For $v_L = c$ we have $\eta = 1$, for v_L given by (3) we have $\eta = 1/3$.

Inserting eq.(4) in the resonant condition (3) and expliciting for the undulator K we obtain a taper scaling which preserves the resonance condition during propagation.

$$K(z)=\sqrt{2\left[\left(\frac{2}{\omega_0}\left(\gamma_s+\alpha\, z\eta\frac{\omega_u}{\omega_0}\right)^2-1\right)\right]} \qquad (5)$$

The correct scaling of the taper depends then on the parameter η, which can be deduced in the more general case of exponential growth in presence of a given taper and energy chirp with the formalism of ref.[20] where the chirped beam evolution has been also studied with the code PROMETEO [21].

We have tested the effect of the tapered undulator with the SPARC FEL operating in velocity bunching mode. The central wavelength used in the experiment is 540 nm and the corresponding β Twiss coefficient is about 1.5m. The mean beam energy measured with the magnetic spectrometer is 116MeV and the emittances measured with the quadrupole scan technique in the transfer line between the linac and the undulator beamline are 2.7/3.0 mm-mrad (x/y). The longitudinal phase space measured with the RF deflector cavity used in combination with the dipole spectrometer is shown in Fig. 14.

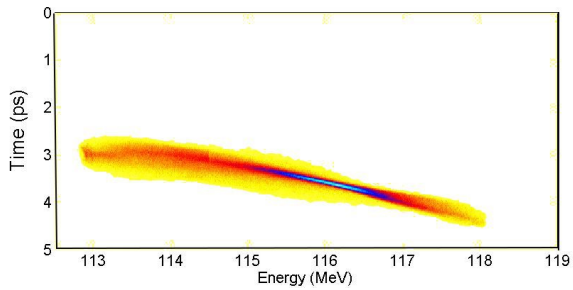

Figure 14: Longitudinal phase space reconstruction at the exit of the linear accelerator.

A list of the beam parameters measured before the injection of the beam in the undulator is presented in Tab.II. The operation in compression mode, i.e. with the first linac section at a phase close to zero crossing, is very sensitive to phase drift and jitter. This is the main reason in the large uncertainty factor in the chirp figure.

Tab. II – Summary of the main beam parameters

Beam energy (MeV)	115.2
Energy Spread (proj., %)	1.15
Energy Spread (slice, %)	0.6
Chirp keV/μm	6±1.5
Length (ps - rms)	0.42
Peak current (A)	380

The radiation diagnostic was the same used in the experiments presented in the previous sections and it is based on the in vacuum spectrometer. In Fig. 15 it is shown a typical spectrum collected with three undulator gaps set to the resonant wavelength of 540nm (at the mean beam energy).

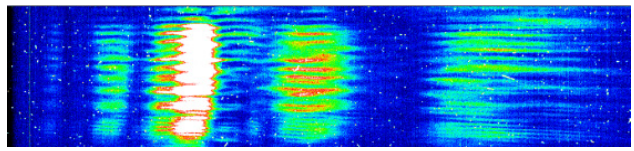

Figure 15: Single shot spectrum acquired with three undulator closed. The vertical axis represents the vertical position at the spectrometer entrance slit. The window is centred at 540nm and the window width is 45nm.

The vertical structure in the spectrum image is due to the radiation diffraction caused by the vacuum pipe. With the first three undulator set at resonance and the last three undulators opened, the radiation has to propagate through about 8 m of vacuum pipe without gain guiding. The structure disappears in Fig. 16, obtained with six sections tuned at the resonance of 540nm (un-tapered undulator).

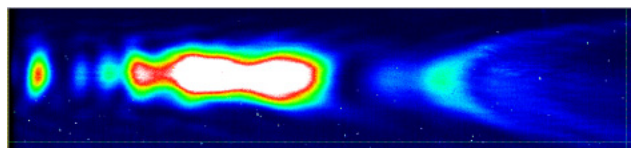

Figure 16: As in Fig. 15, single shot spectrum acquired with six undulators set at the resonance of 540nm.

The strong chirp in the electron bunch shows up as a broadband spectrum filling up the wavelength acceptance window of the spectrometer. A statistical analysis of the collection of 100 spectra acquired in this condition provided the histograms shown in Fig.s 17 and 18.

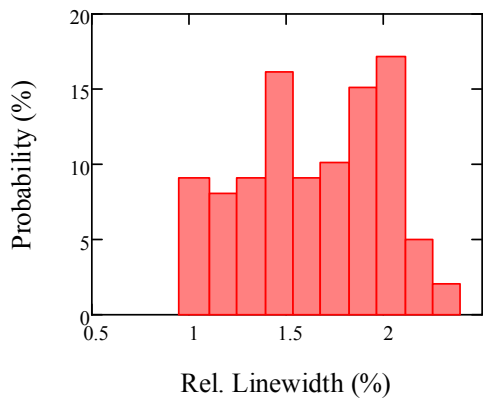

Figure 17: Histogram of the spectral width obtained with the untapered undulator, with the resonance set at 540nm.

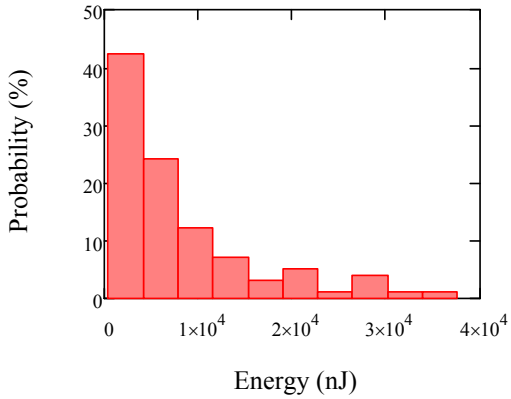

Figure 18: Histogram of the pulse energy obtained with the untapered undulator.

The average pulse energy obtained in these conditions is 7.8μJ. The r.m.s. of the distribution is comparable to the mean value (8 μJ).

The technique used to compensate the chirp with the taper was that of progressively closing the gaps one module at the time, starting from the first one while observing the emitted spectrum. For each module we found the gap minimizing the spectral width. This procedure lead to the set of gaps corresponding to the resonance frequencies (at 115 MeV) shown in Fig. 18.

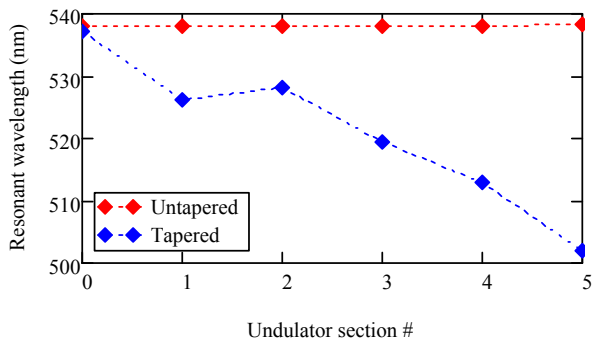

Figure 19: Resonant frequency in the six undulators in the untapered and tapered case.

After the procedure, with the resonant frequency per undulator as shown in Fig.19, we have obtained a substantial increase of the pulse energy which reached 140μJ with a standard deviation of about 100μJ and a reduction of the average linewidth which was $8x10^{-3}$ averaged over 100 pulses. In Fig. 20 and 21 the histograms relevant to the statistics of the pulse energy and relative linewidth for the 100 shots are shown. Several spectra in the acquired set were characterized by a spectral pattern similar to the one shown in Fig. 22, constituted by a single coherence region (no SASE spikes). The pulse energy in the spectrum of Fig.21 is about 260μJ. The red dashed line corresponds to a Gaussian profile fitting the main structure in the spectrum with a spectral width of 1.65nm. A Fourier limited pulse would have an rms length of 46fs and a peak power of about 900MW.

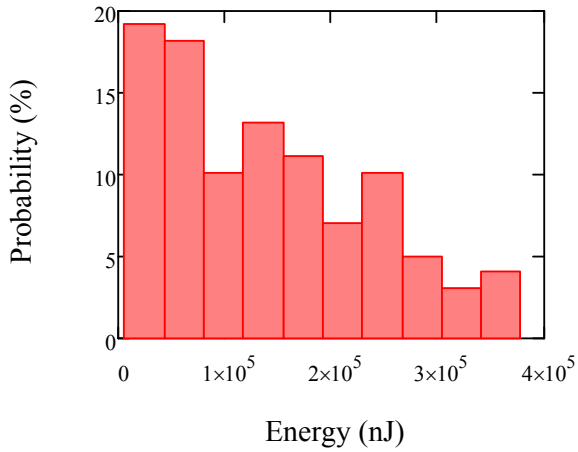

Figure 20: Histogram of the pulse energy obtained with the tapered undulator.

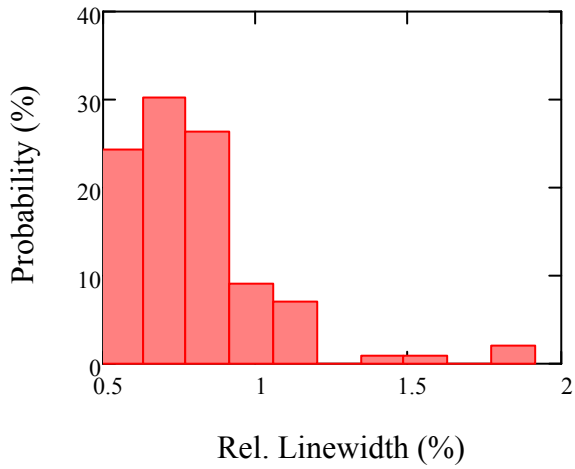

Figure 21: Histogram of the relative linewidth obtained with the tapered undulator.

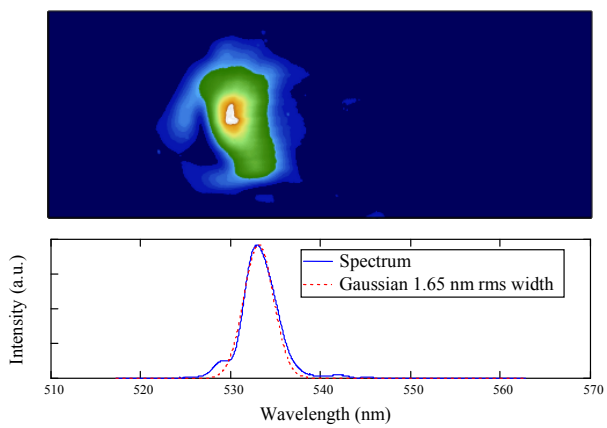

Figure 22: Typical spectrum showing a single coherence region (single spike).

CONCLUSIONS

The SPARC scientific activity encompasses FEL physics and beam dynamics experiments. In this paper we have summarized three of the main recent achievements consisting in the observation of high harmonics emission from a single pass FEL amplifier seeded at saturation levels with an external laser, in the realization of a cascaded FEL operating above saturation with the observation of the third harmonic in the radiator and finally in the operation in SASE mode with a chirped beam compensated by the undulator taper. This is a promising way to obtain short Fourier limited radiation pulses and we have confirmed for the first time the observation of spectra without any typical SASE spiking structure.

REFERENCES

[1] E. L. Saldin, E. A. Schneidmiller, and M.V. Yurkov, PRST-AB 9, 050702 (2006)

[2] M. Ferrario et al, Proc. Of 2009 FEL Conf, Liverpool Jacow - THOB01. See also http://www.sparc.it and http://www.lnf.infn.it/acceleratori/sparc/

[3] L. Giannessi et al. Nuclear Instruments and Methods in Physics Research A 593 (2008) 132– 136

[4] M. Ferrario et al., Phys. Rev. Lett. 104, 054801 (2010)

[5] M. Quattromini et al., Proceedings of EPAC08, Genoa, Italy (2008)

[6] M. Quattromini et al. SPARC Note FEL/09/005, http://www.frascati.enea.it/SPARC/SPARC_FEL_09_005.pdf

[7] L. Ficcadenti et al. Proceedings of PAC07, Albuquerque, New Mexico, USA RF Deflector/ FRPMN030 (2007).

[8] L.Giannessi et al. *These proceedings*

[9] J. R. Pierce, Traveling-Wave Tubes. New York: Van Nostrand, (1950).

[10] S.Reiche, Nucl. Instr. & Meth. A429, 243-248 (1999).

[11] L. Giannessi, P. Musumeci, New J. Phys. 8 (2006).

[12] L. Giannessi, Procs. of the 2006 FEL conference (JACOW), 91-94.

[13] L. Giannessi, P. Musumeci, S. Spampinati, J. Appl. Phys. 98, 043110 (2005).

[14] R. Bonifacio, B.W.J.McNeil, P.Pierini, Phys. Rev. A 40, 4467–4475 (1989).

[15] R. Bonifacio, N. Piovella and B. W. J. McNeil Phys. Rev. A 44, 3441 (1991)

[16] R.Bonifacio et al., Rivista del nuovo cimento 18, 1-69 (1990).

[17] T. Watanabe et al. Phys. Rev. Lett. **98,** 034802 (2007)

[18] L. H. Yu et al. Science 289, 932-934 (2000).

[19] S.J.Hahn, J.K. Lee, Phys. Rev. E 48, 2162-2171 (1993).

[20] G. Dattoli L. Giannessi, P. L. Ottaviani and S. Pagnutti MOPB16, *These proceedings*

[21] G. Dattoli, M. Galli, P.L. Ottaviani, ENEA Internal Report RT/INN/93/09, 1993.